

## Insights into the Electronic Properties of Coumarins: A Comparative Study

R. Giri<sup>a</sup> and R. Payal<sup>b,\*</sup>

<sup>a</sup>Department of Physics and Electronics, Rajdhani College, University of Delhi, Delhi-110015, India

<sup>b</sup>Department of Chemistry, Rajdhani College, University of Delhi, Delhi-110015, India

(Received 14 February 2022, Accepted 11 June 2022)

The effect of substitution on some biologically active di- and tri-coumarins substituted 4-phenyl coumarins were investigated using absorption and fluorescence spectrum profiles. These studies helped in the estimation of excited-state dipole moments ( $\mu_e$ ) of coumarins by applying two renowned Solvatochromic shift methods: Kawaski *et al.* and Ravi *et al.* Computational methodology was applied to find the ground state dipole moments ( $\mu_g$ ) and Onsager cavity of the coumarins from the optimized geometry of the molecules using DFT/B3LYP/6-31++ G(d,p) level of theory. The Mulliken charges, frontier molecular orbitals (FMO), and electrostatic potential surfaces (EPS) were theoretically generated utilizing their optimized geometries to validate the experimental findings. Time Dependent Density Functional Theory (TD-DFT) approach was applied to approximate the excitation energy, dispersion energy, cavitation energy, corresponding wavelengths, and oscillator strength for different coumarins in the gaseous phase in addition to benzene, ethanol, and most polar aqueous medium. The large stoke's shifts and high  $\mu_e$  values indicate that the intramolecular charge transfer (ICT) process occurs in these coumarins which have coerced by an intense  $S_0 \rightarrow S_1$  electronic transition. The computational results were matched with the experimental analysis, and revealed characteristics electrical properties of coumarins, as well as confirming the presence of ICT in these coumarins.

**Keywords:** Solvent effect, TD-DFT calculations, Molecular orbitals, Oscillator strength, ICT

### INTRODUCTION

Coumarins (1-benzopyran-2-ones) are an interesting class of biologically active molecules containing the benzene ring fused with a hexagonal lactone ring and are found in variety of bacteria, fungi, and plants [1]. Because of the lipophilic, planar, and aromatic 2H-chromen-2-one ring, they are amphiphilic in nature and interact with a variety of lipophilic biological equivalents *via* strong hydrophobic, and  $\pi$ - $\pi$  stacking interactions. Coumarins have a hydrophilic lactone group that confers strong polar binding to the molecule, such as hydrogen bonds and dipole-dipole interactions. Coumarins with potent backbones have been a subject of continuous exploration by various research groups and novel synthetic pathways and protocols are designed

from time to time [2-6]. This versatility in the chemical structure of coumarins caused by substitution can have a significant impact on the photochemical characteristics of the compound [7,8].

These extensive claims are meticulously relevant to their photophysical processes such as intramolecular charge transfer (ICT) which is highly sensitive to solvent polarity as well as its structure in both ground and excited states. Coumarins have amazing fluorescence properties, including high sensitivity to their local environment, such as polarity and viscosity, which explains why solvents have such a strong influence on their chemical and physical properties, causing changes in their electronic transitions (*aka* solvatochromism) [9-13]. This makes absorption and fluorescence spectroscopy useful for estimating various photophysical parameters of coumarins in their ground and excited states [14-19].

\*Corresponding author. E-mail: ritupayal@rajdhani.du.ac.in

Excited states play a prominent role in photoinduced reactions, as well as in cases where only the ground state is present. The excitation spectra describe the various transitions that occur during the excitation of a molecule from its ground to excited state. The transitions between energy levels of an atom or molecule, and oscillator strength ( $f$  value) determines the likelihood of electromagnetic radiation absorption or emission. In quantum chemistry, the time-dependent density functional theory (TD-DFT) is getting a lot of traction as an expedient tool for approximating various excited state electronic properties. The excitation spectra and the dipole oscillator strengths are obtained by means of the TD-DFT approximation [20]. Different parameters induced by solute-solvent interactions such as excited state energy ( $E_{\text{exc}}$ ), dispersion energy ( $E_{\text{dis}}$ ), cavitation energy ( $E_{\text{cav}}$ ), repulsion energy ( $E_{\text{repul}}$ ), non-electrostatic energy ( $E_{\text{non-el}}$ ), polarized solute-solvent interaction energy ( $E_{\text{PSS}}$ ), free energy of solvation ( $\Delta G_{\text{sol}}$ ), and various other properties of the molecule in its excited state are estimated [21,22].

In the present work, seven coumarins with various groups were chosen to investigate the effects of solvent polarity and substitution on dynamic processes in order to reveal their photon-induced charge transfer mechanism using absorption and fluorescence spectral profiles, as well as computational DFT approach. Experimentally, using solvatochromic shift approaches the ratio of dipole moment ( $\mu_e/\mu_g$ ) and change in dipole moment ( $\Delta\mu$ ), are estimated which are then utilized to estimate the excited-state dipole moments ( $\mu_e$ ) of distinct coumarins using their theoretically calculated ground state dipole moments. Furthermore, theoretically analyzed characteristics such as frontier molecular orbital (FMO) diagrams, electrostatic potential (ESP) energy maps, Mulliken charges, as well as excitation energy ( $E_{\text{exc}}$ ) and oscillator strengths ( $f$  values) derived by TD-DFT calculations have been used to validate the experimental results.

## EXPERIMENTAL

### Materials

The coumarins under study were received from Late Prof. V.V.S. Murti (Department of Physics and Astrophysics, University of Delhi) who is co-author of many research papers on coumarins and used as such [23]. The solvents used

were spectroscopic and HPLC quality with 99.5-99.8 purity from Merck and were checked for impurities in the scanning range. The spectral solutions were made with triple distilled water and a variety of solvents such as benzene, 1-butanol, 1,4-dioxane, ethanol, N,N-dimethylformamide, propanol, and methanol.

### Instrumentation

Coumarin's absorption and fluorescence spectra were obtained at room temperature with matching quartz cuvettes in solvents of various polarity and hydrogen bonding abilities using Shimadzu-260 spectrophotometer and Aminco-Bowman Spectrofluorometer, respectively. To avoid aggregation and decrease inner filter effects, the solute concentration was fixed at  $10^{-6}$  M.

## METHODS: DETERMINATION OF EXCITED STATE DIPOLE MOMENT

### Theoretical Calculations and Geometry Optimization

The results of geometry optimization on the coumarins are listed in Tables S1-S3. All theoretical calculations are carried out using quantum chemical package GaussView [24] using DFT and TD-DFT approaches using B3LYP with 6-31++G(d,p) theory to cast more light on the observed experimental phenomena and provide a reasonable explanation. To corroborate the experimental data, TD-DFT calculations were performed using implicit solvation model namely, Integral equation formalism polarizable continuum model (IEFPCM) [25] in benzene, ethanol, and water. The energies were minimized with regard to all geometrical parameters, ignoring molecular symmetry requirements, to optimize geometries.

The bond lengths ( $\text{\AA}$ ) and bond angles ( $^\circ$ ) of the coumarins were obtained from their optimized geometries. The  $\text{C}_3=\text{C}_4$  bond length of coumarins was found to be in the range 1.343-1.364  $\text{\AA}$  and was comparable to that of the  $\text{C}=\text{C}$  bond of ethene (1.34  $\text{\AA}$ ) molecule indicating minimal delocalization in this bond. The  $\text{C}_2-\text{C}_3$  bond lengths were constrained to 1.442-1.536  $\text{\AA}$ ,  $\text{C}_4-\text{C}_{10}$  bond lengths were in the range 1.448-1.532  $\text{\AA}$ , and  $\text{C}_4-\text{C}_{13}$  ( $\text{C}_{13}$  is the carbon atom of methyl substituent at 4<sup>th</sup> position) bond lengths were in scale 1.507-1.540  $\text{\AA}$  (Table S1). The  $\text{C}_2-\text{C}_3$  and  $\text{C}_4-\text{C}_{10}$  bond lengths were slightly lower than the C-C bond length of

ethane (1.54 Å) because these bonds are involved in the ICT process thereby, fluctuating the actual bond length value. However, the C<sub>4</sub>-C<sub>13</sub> bond length is approximately equal to 1.54 Å as this bond is present outside the pyranone ring and is not contributing to ICT. The bond lengths of the atoms present in the benzene ring are ~1.4 Å indicating these bonds are neither pure single nor pure double bond because of resonance the benzene ring is showing a Kekule structure. The C-H, C-O, and C=O bond lengths are in the range 1.07-1.096 Å, 1.316-1.426 Å, 1.220-1.258 Å which are in perfect agreement with the literature value of ~1.09 Å, ~1.43 Å, and ~1.2 Å, respectively.

The bond angles of different bonds of coumarins are listed in Tables S2 and S3. The bond angles of the benzene ring and pyranone ring of all C-C-C bonds are found to be ~120°. The bond angle O<sub>1</sub>-C<sub>2</sub>-C<sub>3</sub> is in the range 114.66-121.19° which is approximately equal to the literature value of ~111°. The bond angle O<sub>1</sub>-C<sub>2</sub>-O<sub>11</sub> varies in the range 115.63-119.39° however the actual value is 120°. The C-O-H bond angle in C-1 is 103.22° which is justifying a literature value of 109°. The bond lengths and bond angles values obtained from the optimized geometries of the coumarins matched with their literature values and gave idea about the nature of bonds. These optimized geometries were also used to calculate the Onsager cavity radii (a) and ground state dipole moments (μ<sub>g</sub>) of coumarins which are used to determine the excited state dipole moments.

### Excited-state Dipole Moments: Experimental Approach

The position of the absorption and fluorescence bands is influenced by the electric field, which affects the dipole moment of a molecule in its excited state. Currently, we are analyzing the properties of seven coumarins using two methodologies that rely on the internal electric field. In a previous paper, a full explanation of these strategies was discussed [26].

**Dipole moments using Kawski *et al.* model.** The nature of the solvent influences the absorption and fluorescence spectra, which allows the determination of dipole moments in their excited states. We adopted a model provided by Bilot and Kawski for this purpose, which is based on bulk polarity constraints:  $f(\epsilon, n)$  and  $\varphi(\epsilon, n)$  (tabularized in Table 1) [27]. Kawski and coworkers [28-32] gave two formulas (Eqs. (1) and (2)) involving wavenumbers of absorption ( $\bar{\nu}_a$ ) and fluorescence ( $\bar{\nu}_f$ ) spectral bands in a range of solvents, using quantum mechanical perturbation theory of the interaction between a solvent and spherical solute and subsuming Onsager's model [33] as:

$$\bar{\nu}_a - \bar{\nu}_f = m_1 f(\epsilon, n) + \text{const} \quad (1)$$

$$\bar{\nu}_a + \bar{\nu}_f = -m_2 \varphi(\epsilon, n) + \text{const} \quad (2)$$

where  $\bar{\nu}_a - \bar{\nu}_f$  and  $\bar{\nu}_a + \bar{\nu}_f$  are spectral shifts (cm<sup>-1</sup>),  $\epsilon$  and

**Table 1.** Solvent Polarity Parameters ( $E_T^N, f(\epsilon, n), \varphi(\epsilon, n)$ ) for Different Solvents Used in Present Study

Solvent <sup>a</sup>	$\epsilon$	$n$	$E_T^N$	$f(\epsilon, n)$	$\varphi(\epsilon, n)$
Benzene	2.30	1.5000	0.111	0.005	0.340
1,4-Dioxane	2.21	1.4224	0.164	0.040	0.310
DMF	6.71	1.4305	0.386	0.840	0.710
2-Propanol	19.92	1.3772	0.546	0.780	0.646
1-Butanol	19.92	1.3772	0.586	0.750	0.647
Ethanol	24.30	1.3610	0.654	0.813	0.653
Methanol	32.66	1.3284	0.762	0.855	0.650
Water	78.36	1.3330	1.000	0.913	0.683

<sup>a</sup>Solvents are arranged in order of increasing  $E_T^N$  values.

$n$  are solvent's dielectric constant, and refractive index, respectively. The slopes  $m_1$  and  $m_2$  (Eqs. (3a) and (3b), respectively), obtained by plotting  $(\bar{V}_a - \bar{V}_f)$  versus  $f(\epsilon, n)$  and  $(\bar{V}_a + \bar{V}_f)$  versus  $\varphi(\epsilon, n)$ , respectively are given as:

$$m_1 = \frac{2(\mu_e - \mu_g)^2}{hca^3} \quad (3a)$$

$$m_2 = \frac{-2(\mu_e^2 - \mu_g^2)}{hca^3} \quad (3b)$$

where 'a',  $\mu_g$ , and  $\mu_e$  denote Onsager cavity radius, ground- and excited state dipole moments, respectively of the molecule under study. Because 'a' is constant in both the ground and excited states, dividing  $m_1$  by  $m_2$  yields the ratio of excited to ground state dipole moment as:

$$\frac{\mu_e}{\mu_g} = \left( \frac{m_1 + m_2}{m_2 - m_1} \right) \quad (m_1 < m_2) \quad (4)$$

**Dipole moments using Ravi *et al.* Model.** For the estimation of spectral shifts with  $E_T^N$ , Ravi *et al.* [34] used a theoretical method for determining the Onsager cavity radii 'a'. This approach produces more precise findings because the ratio of two Onsager radii ( $a_B/a$ ) is taken into account (Eq. (5)):

$$\bar{V}_a - \bar{V}_f = 11307.6 [(\Delta\mu/\Delta\mu_B)^2 (a_B/a)^3] E_T^N + \text{constant} \quad (5)$$

The plot of  $(\bar{V}_a - \bar{V}_f)$  vs.  $E_T^N$  gives  $\Delta\mu$  using slope 'm<sub>3</sub>' (Eq. (6)) which is given as:

$$\text{slope } (m_3) = 11307.6 \left[ \left( \frac{\Delta\mu}{\Delta\mu_B} \right)^2 \left( \frac{a_B}{a} \right)^3 \right] \quad (6)$$

where  $(\bar{V}_a - \bar{V}_f)$  denotes Stokes-shift of the solute in different solvents.  $\Delta\mu_B (= 9D)$  and  $\Delta\mu$  designates change in dipole moment of betaine dye and solute, respectively on excitation.  $a_B (= 6.2 \text{ \AA})$  and 'a' are the Onsager cavity radius of betaine dye and coumarins, respectively [35].  $E_T^N$  reflects the solvent polarity parameter recommended by Reichardt

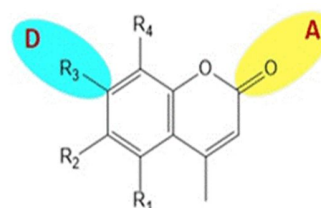
and coworkers [36-38], which is connected to the absorption spectra of betaine dye in the solvent. The  $E_T^N$  values for the solvents employed in the present study are mentioned in Table 1. The Onsager cavity radii of coumarins were taken as 40% of the longest axis using their optimized geometries [26,39]. As a result, estimation of  $\mu_g$  and 'a' values *via* computational calculations allows the calculation of  $\mu_e$ .

## RESULTS AND DISCUSSION

Coumarins (C-1 to C-7) with various benzene ring substitution groups were chosen to explore their photophysical activity. In terms of substituents, C-1 to C-3 differ from C-4 to C-7 in that the former are di-substituted while the latter are tri-substituted (Fig. 1). The absorption and fluorescence spectra of coumarins are studied in different solvents and are shown in Figs. 2 and 3.

### Absorption Spectral Properties

The absorption and fluorescence spectra of coumarins were examined in solvents with different polarities (Table 1) and the corresponding band maxima were tabulated in Tables 2 and 3. The absorption spectra of coumarins (Fig. 2a for C-1 and Fig. 3a for C-5) exhibit one shoulder peak in the UV-Vis region ~280-310 nm, and two well-defined peaks in region ~235-250 nm and ~315-370 nm, respectively under



Molecules	Label	R <sub>1</sub>	R <sub>2</sub>	R <sub>3</sub>	R <sub>4</sub>
4-methyl-7-hydroxy coumarin	C-1	H	H	OH	H
4-methyl-7-amino coumarins	C-2	H	H	NH <sub>2</sub>	H
4-methyl-7-methoxy coumarin	C-3	H	H	OCH <sub>3</sub>	H
4-methyl-5,7-diethoxy coumarin	C-4	OC <sub>2</sub> H <sub>5</sub>	H	OC <sub>2</sub> H <sub>5</sub>	H
4-methyl-6,7-diethoxy coumarin	C-5	H	OC <sub>2</sub> H <sub>5</sub>	OC <sub>2</sub> H <sub>5</sub>	H
4-methyl-6,7-dihydroxy coumarin	C-6	H	OH	OH	H
4-methyl-7,8-diethoxy coumarin	C-7	H	H	OC <sub>2</sub> H <sub>5</sub>	OC <sub>2</sub> H <sub>5</sub>

**Fig. 1.** Different coumarins employed in present study.

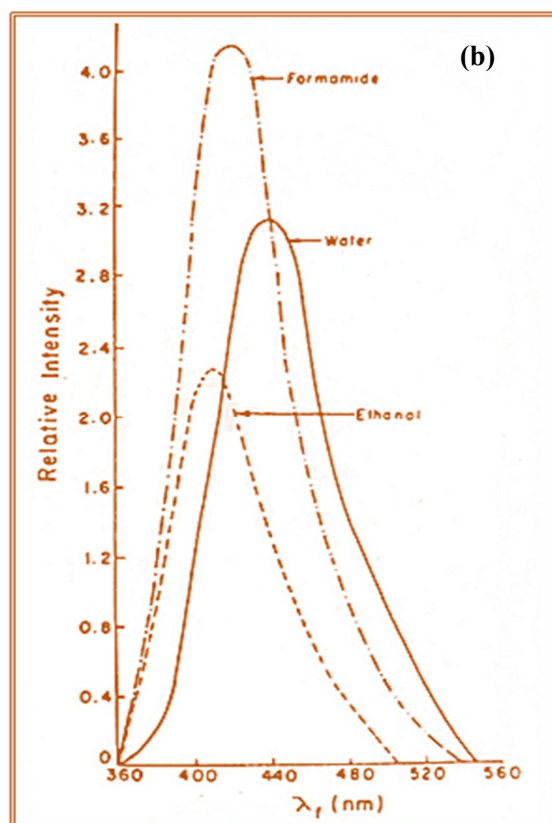
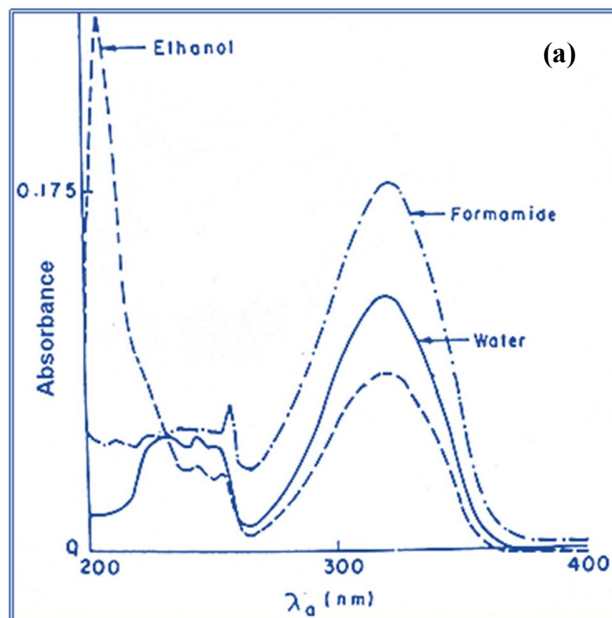
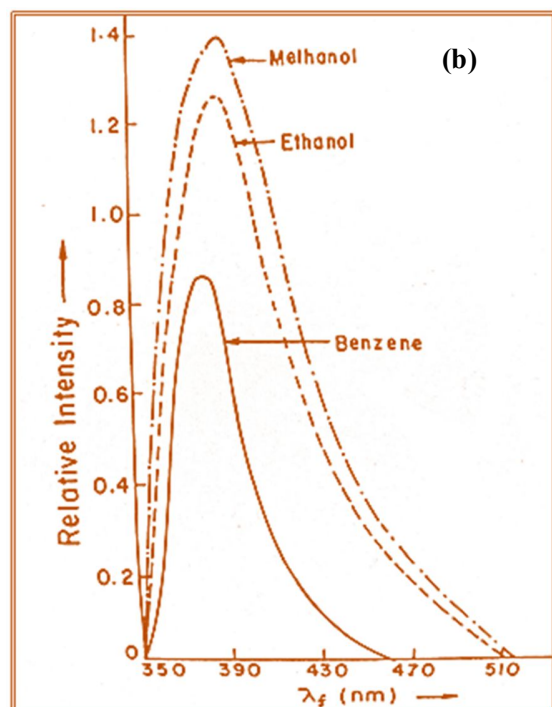
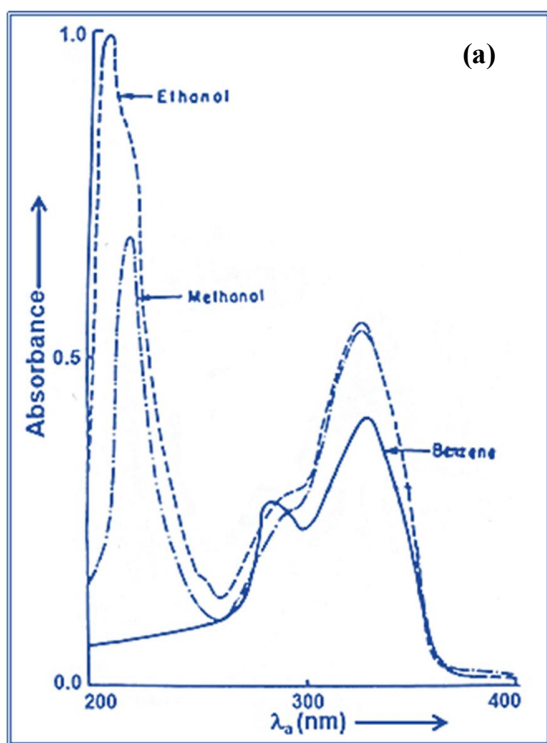


**Fig. 2.** (a) Absorption spectra of C-1 in benzene, ethanol, and methanol. (b) Fluorescence spectra of C-1 in benzene, ethanol, and methanol.

**Fig. 3.** (a) Absorption spectra C-5 in formamide, ethanol, and water. (b) Fluorescence spectra of C-5 in formamide, ethanol, and water.

**Table 2.** Absorption ( $\lambda_a$ ) Band Maxima (in nm) of Coumarins in Different Solvents

Solvent <sup>a</sup>	C-1	C-2	C-3	C-4	C-5	C-6	C-7
	$\lambda_{a1}, \lambda_{a2}, \lambda_{a3}^b$	$\lambda_{a1}, \lambda_{a2}, \lambda_{a3}$	$\lambda_{a1}, \lambda_{a2}, \lambda_{a3}$	$\lambda_{a1}, \lambda_{a2}, \lambda_{a3}$	$\lambda_{a1}, \lambda_{a2}, \lambda_{a3}$	$\lambda_{a1}, \lambda_{a2}, \lambda_{a3}$	$\lambda_{a1}, \lambda_{a2}, \lambda_{a3}$
Benzene	-, 285, 320	-, 300, 345	-, 285, 319	-, -, 319	-, -, 315	-, 305, 348	-, -, 315
1,4-Dioxane	-, 283, 323	-, 305, 350	-, 282, 320	-, -, 320	-, -, 318	268, 322, 350	-, 258, 316
DMF	-, 305, 325	-, 308, 351	-, -, 322	-, -, 322	-, -, 322	278, 325, 353	-, -, 317
n-Propanol	226, 295, 324	225, 306, 352	242, 286, 321	-, 230, 322	-, 232, 320	267, 305, 353	220, 254, 319
1-Butanol	226, 296, 325	225, 306, 354	242, 287, 322	-, 230, 321	-, 232, 321	267, 306, 345	220, 254, 317
Ethanol	228, 295, 324	227, 307, 354	246, 287, 320	212, 235, 320	213, 232, 320	268, 310, 346	220, 254, 318
Methanol	230, 298, 323	227, 308, 351	246, 287, 320	212, 236, 320	213, 235, 320	270, 312, 350	220, 255, 318
Water	232, 298, 322	230, 310, 362	248, 290, 321	210, 240, 323	215, 240, 323	274, 312, 348	210, 255, 320

<sup>a</sup>Solvents are arranged in order of increasing  $E_T^N$  values. <sup>b</sup>absorption band maxima ( $\lambda_{a1}, \lambda_{a2}, \lambda_{a3}$ ).

**Table 3.** Fluorescence Band Maxima (in nm) of Coumarins in Different Solvents

Solvent <sup>a</sup>	C-1	C-2	C-3	C-4	C-5	C-6	C-7
Benzene	377 <sup>b</sup>	402	379	391	392	NF <sup>c</sup>	NF
1,4-Dioxane	380	407	372	408	395	470	468
DMF	388	440	386	418	413	483	475
n-Propanol	388	433	385	408	404	477	454
1-Butanol	388	430	382	408	408	477	355
Ethanol	387	435	382	410	410	476	465
Methanol	389	437	382	417	417	475	472
Water	451	446	386	437	437	484	506

<sup>a</sup>Solvents are arranged in order of increasing  $E_T^N$  values. <sup>b</sup> $\lambda_{a3}$  is the excitation wavelength. <sup>c</sup>Non-fluorescent.

the effect of alteration of substituent at benzene ring and varying solvents polarity. The shorter absorption band can be allocated to the  $\pi$ - $\pi^*$  transition of the benzene ring, whereas

the longest wavelength band confers the interaction of the benzene ring with the pyranone moiety giving  $\pi$ - $\pi^*$  transitions. The broad, asymmetric shoulder band represents

(in the region  $\sim 300$  nm) two overlapping  $\pi$ - $\pi^*$  transitions (Fig. 2). There are no  $n$ - $\pi^*$  transitions because they are likely screened by the more intense  $\pi$ - $\pi^*$  transitions ( $\epsilon_m \approx 10^2 \text{ M}^{-1} \text{ cm}^{-1}$ ). The bands are labeled in accordance with the literature [9,15,40].

The coumarins band maxima changed slightly (by 2-3 nm) as the polarity of the solvents changed from benzene to water, showing that the ground state of coumarins is unaffected by the change in solvents and confirming weaker solute-solvent interactions (Table 2). When di-substituted coumarins: C-1, C-2, and C-3 (with  $R_3 = -\text{OH}$ ,  $-\text{NH}_2$ ,  $-\text{OCH}_3$ ) were moved towards the most polar solvent under study (*i.e.* water), a blue shift was detected. A strong hydrogen bonding between the non-bonded electron pairs of the  $R_3$  group and  $\text{H}_2\text{O}$  molecules stabilizes the LUMO more resulting in an increase in the energy gap between HOMO and LUMO, justifying the peculiar behavior [9,26].

The absorption band maxima for di-substituted coumarins shift towards the longer wavelength side when the substitution at  $R_3$  (7<sup>th</sup> position of coumarins) is modified according to the following:  $-\text{NH}_2 > -\text{OH} > -\text{OCH}_3$ . This behavior holds good in all solvents regardless of the polarity, refractive index, and viscosity. Interestingly, the substitution of benzene with functional groups such as  $-\text{NH}_2$  ( $\lambda_{\text{max}} = 284$  nm),  $-\text{OH}$  ( $\lambda_{\text{max}} = 272$  nm), and  $-\text{OCH}_3$  ( $\lambda_{\text{max}} = 269$  nm) also follow a similar pattern. The tri-substituted coumarins with ethoxy or hydroxyl groups at different locations also suffer a similar behavior. The absorption band maxima of coumarin with two hydroxyl groups (C-6) displays a greater shift in wavelength than the coumarins having two ethoxy groups (C-4, C-5) as the former is more polar (Table 2).

### Fluorescence Spectral Properties

For all of the computations presented here, the longest wavelength absorption band maxima ( $\lambda_{\text{a3}}$ ) is used as excitation wavelength (in the range of 315-370 nm). Fluorescence spectra of coumarins in all solvents display a single fluorescence band. The fluorescence spectra of C-1 and C-5 are displayed in Figs. 2b and 3b. With increasing solvent polarity from benzene to water, the fluorescence band is detected in the region of 380-560 nm and experiences a bathochromic shift of  $\sim 14$ -74 nm. In comparison to other solvents, water molecules stabilize the excited state more and reduce the energy difference between ground and excited

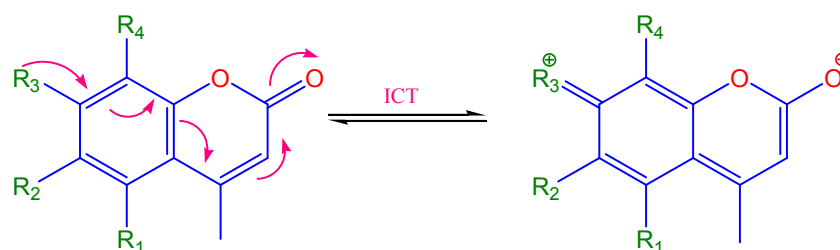
states, resulting in a large bathochromic shifted broad structureless band for coumarins. The presence of non-bonding electrons in C-1 to C-3 due to the inclusion of a strong electron donating group such as  $-\text{OH}$ ,  $-\text{NH}_2$ ,  $-\text{OCH}_3$  enhances electron transfer to the other end of the molecule, raising band maxima and relative fluorescence intensity. More noteworthy features are revealed when another functional group is introduced at the 5-, 6-, or 8-positions of coumarins to produce tri-substituted coumarins (C-4, C-5, C-6, and C-7). Furthermore, the bandwidth of all coumarins was found to increase as the polarity of the solvents increased. However, more specific interactions of tri-substituted coumarins (C-4 to C-7) with solvents lead to a wider bandwidth with more red shift than di-substituted coumarins C-1 to C-3 (Table 3). The comparative lower  $\epsilon_m$  value of coumarins with polar groups in the most polar solvent (water) also supports the fact (Table 4).

The substantial Stoke shifts and high relative fluorescence indicate that the excited state has been stabilized more due to strong interactions between the coumarins and the solvents. These properties suggest that in their excited state, coumarins undergo intramolecular charge transfer (ICT) characteristics. Surprisingly, C-6 differs from other coumarins in terms of a noticeable red shift in its band maxima due to the substitution of another polar  $-\text{OH}$  group at the 6<sup>th</sup> position providing additional polarity to C-6. Because the oxygen atom develops a significant negative charge, it accelerates H-bonding in C-6 in polar solvents, resulting in an additional red shift in its band maxima when compared to normal ICT-induced red shifts [23]. In addition to solute-solvent interactions, intramolecular hydrogen bonding may hinder charge mobility to the other parts of the ring due to steric hindrance in the 6<sup>th</sup> and 7<sup>th</sup> positions [41]. C-4, C-5, and C-7 show similar steric crowding, but there is no competition from intramolecular hydrogen bonding in these compounds. These findings convincingly demonstrate that substitution changes in coumarins significantly modify their characteristics in the excited state.

These substituents favor ICT process in coumarins by delocalizing electrons from the  $R_3$  group of the benzene ring to the oxygen atom on the carbonyl group of the pyranone ring, making them positive and negative centers, respectively (Fig. 4). The literature backs up the ICT mechanism [8,9,42].

**Table 4.** Bandwidth ( $\sigma$ ) and Molar Extinction Coefficient ( $\epsilon_m \times 10^2$ ) of Coumarins in Excited State in Different Solvents

Solvent	C-1		C-2		C-3		C-4		C-5		C-6		C-7	
	$\sigma$	$\epsilon_m$	$\sigma$	$\epsilon_m$	$\sigma$	$\epsilon_m$	$\sigma$	$\epsilon_m$	$\sigma$	$\epsilon_m$	$\sigma$	$\epsilon_m$	$\sigma$	$\epsilon_m$
Benzene	27	1.59	26	1.59	30	0.90	36	0.96	26	2.08	24	0.39	28	1.78
1,4-Dioxane	27	1.56	25	1.56	31	0.96	38	0.98	31	2.11	24	0.39	32	1.68
DMF	27	1.28	27	1.28	27	1.04	41	1.11	28	2.97	25	0.45	33	1.79
n-Propanol	26	1.41	26	1.37	27	1.35	38	0.99	26	3.02	24	0.44	33	1.75
1-Butanol	26	1.27	26	1.27	25	1.39	39	1.06	29	3.27	24	0.40	33	1.77
Methanol	28	1.59	27	1.59	31	1.15	40	1.04	28	2.87	25	0.70	32	1.78
Ethanol	26	1.49	26	1.29	25	1.48	40	0.99	28	2.90	23	0.55	33	1.86
Water-	31	1.29	28	1.29	25	1.00	46	0.92	28	2.93	28	0.36	35	2.08

**Fig. 4.** Possible ICT mechanisms shown by coumarins.

### Computational DFT Studies

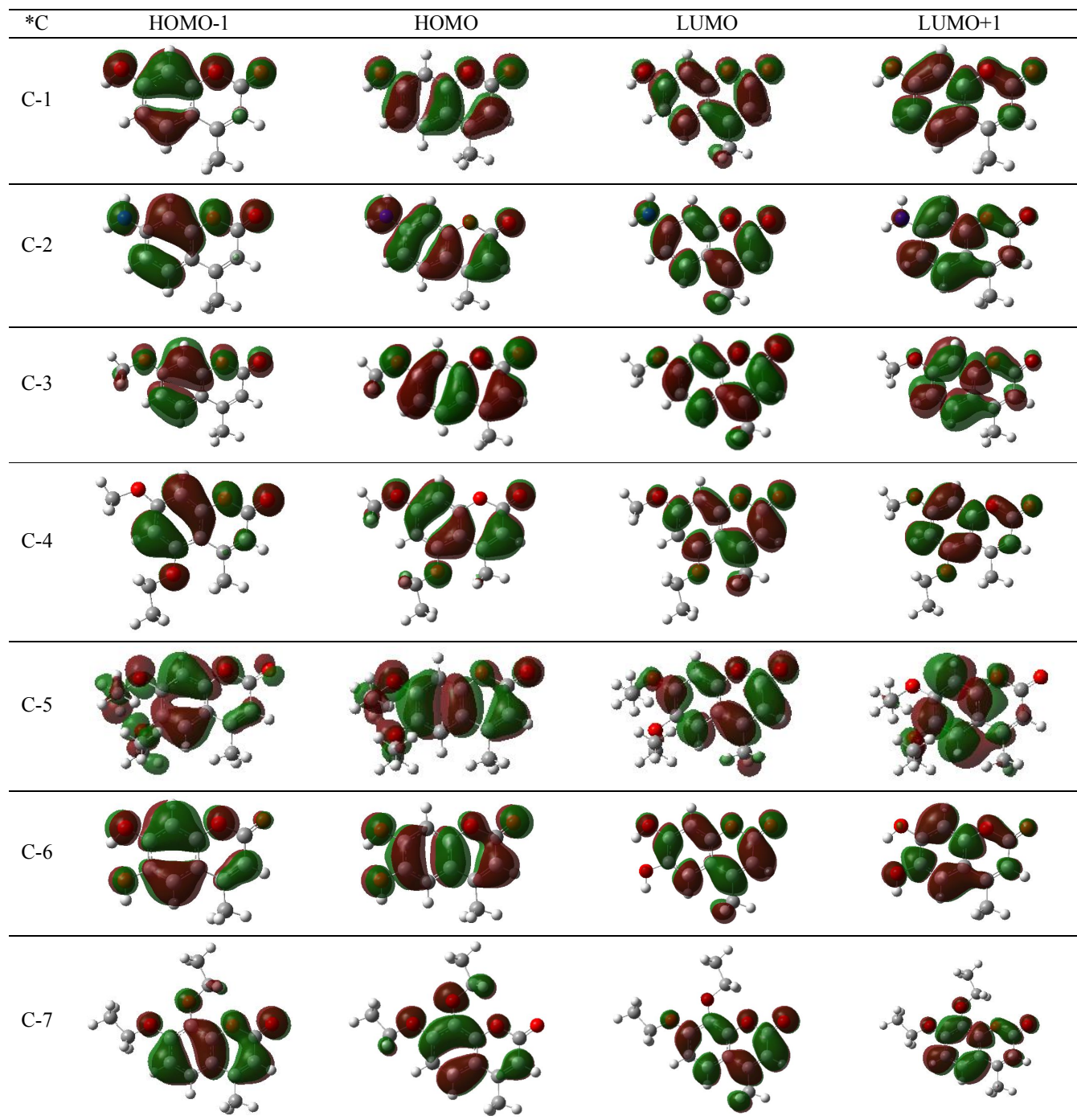
The ICT is further validated *via* computational studies in terms of Mulliken atomic charges (Table 5), Frontier molecular orbital graphs (Fig. 5), and molecular electrostatic potential (ESP) maps (Fig. 6) generated by DFT studies on their optimized geometries.

**Molecular orbitals, electrostatic potential surfaces, and mulliken charges.** The molecular orbitals are crucial because they are linked to excitation features like electronic transitions contribution, excitation energy, donor-acceptor relationship, and band gap [43]. The HOMO and LUMO represent the ability to donate and accept electron, respectively. The energies of molecular orbitals HOMO-1, HOMO, LUMO, and LUMO+1 of coumarins were calculated using B3LYP/6-311++G(d,p) highlighting their excitation transitions (Fig. 5). HOMO and LUMO represent the localization of the electron density on the whole molecule with opposite direction counters, therefore, HOMO-1 and LUMO+1 are also visualized to observe the transference of

charge density. HOMO-1 shows the electron density is mostly concentrated on the benzene ring, whereas in LUMO, the electron density is localized more on the pyranone ring. As a result, the electronic transition from HOMO to LUMO permits charge transfer from the benzene ring's  $R_3$  group (donor) to the pyranone analogue (acceptor) of the molecules justifying the ICT process [44-46]. As a result, the HOMO  $\rightarrow$  LUMO excitations can be classified as  $\pi$ - $\pi^*$  transitions.

The energies of HOMO and LUMO as well as the band gap ( $\Delta E$ ) for coumarins have been estimated theoretically from the HOMO and LUMO plots (Table 6). The energy gap between HOMO and LUMO orbitals can be used to predict the strength, stability, and charge transfer characteristics of the molecules. The energy band gap is found to be in the range of 2.966 eV-4.408 eV for the coumarins. Out of all the coumarins the C-1 has the lowest band gap (2.966 eV) compared to others as C-1 is more polarized, facilitating ICT by a substantial amount of charge transfer from the electron-

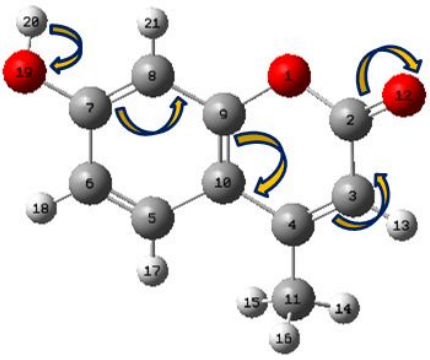




**Fig. 5.** Frontier Molecular Orbitals (HOMO-1, HOMO, LUMO, LUMO+1) of coumarins with isosurface value of  $\pm 0.02$ . \*C corresponds to different coumarins

donating group ( $-OH$ ) to the proficient electron-acceptor groups ( $-C=O$  group of pyranone ring). All other coumarins

have a band gap in the range 4.408-4.146 eV (Table 4) which explains the subsequent charge transfer interaction within

**Table 5.** Mulliken Charges on Selected Atoms of Coumarins Involved in ICT


C-1		C-2		C-3		C-4		C-5		C-6		C-7	
A <sup>a</sup>	q <sup>b</sup>	A	q	A	q	A	q	A	q	A	q	A	q
H <sub>20</sub>	0.342	H <sub>20</sub>	0.309	H <sub>21</sub>	0.156	H <sub>21</sub>	0.158	H <sub>21</sub>	0.189	H <sub>20</sub>	0.392	H <sub>21</sub>	0.158
O <sub>19</sub>	-0.467	N <sub>19</sub>	-0.651	C <sub>20</sub>	-0.146	C <sub>20</sub>	-0.121	C <sub>20</sub>	-0.190	O <sub>19</sub>	-0.526	C <sub>20</sub>	0.014
C <sub>7</sub>	-0.189	C <sub>7</sub>	0.168	O <sub>19</sub>	-0.305	O <sub>19</sub>	-0.359	O <sub>19</sub>	-0.300	C <sub>7</sub>	0.357	O <sub>19</sub>	-0.148
C <sub>8</sub>	-0.555	C <sub>8</sub>	-0.713	C <sub>7</sub>	-0.526	C <sub>7</sub>	-0.222	C <sub>7</sub>	0.309	C <sub>8</sub>	-0.705	C <sub>7</sub>	-0.274
C <sub>9</sub>	-0.321	C <sub>9</sub>	-0.416	C <sub>8</sub>	-0.746	C <sub>8</sub>	-0.862	C <sub>8</sub>	-0.800	C <sub>9</sub>	-0.389	C <sub>8</sub>	-0.248
C <sub>10</sub>	0.819	C <sub>10</sub>	0.782	C <sub>9</sub>	-0.526	C <sub>9</sub>	-0.474	C <sub>9</sub>	-0.514	C <sub>10</sub>	0.669	C <sub>9</sub>	-0.316
C <sub>4</sub>	0.928	C <sub>4</sub>	0.998	C <sub>10</sub>	0.964	C <sub>10</sub>	-0.098	C <sub>10</sub>	0.844	C <sub>4</sub>	1.265	C <sub>10</sub>	0.656
C <sub>3</sub>	-0.592	C <sub>3</sub>	-0.670	C <sub>4</sub>	0.950	C <sub>4</sub>	1.361	C <sub>4</sub>	0.627	C <sub>3</sub>	-0.699	C <sub>4</sub>	1.139
C <sub>2</sub>	0.576	C <sub>2</sub>	0.649	C <sub>3</sub>	-0.686	C <sub>3</sub>	-0.586	C <sub>3</sub>	-0.430	C <sub>2</sub>	0.647	C <sub>3</sub>	-0.893
O <sub>12</sub>	-0.449	O <sub>12</sub>	-0.470	C <sub>2</sub>	0.582	C <sub>2</sub>	0.726	C <sub>2</sub>	0.591	O <sub>12</sub>	-0.464	C <sub>2</sub>	0.346
O <sub>1</sub>	-0.381	O <sub>1</sub>	-0.432	O <sub>12</sub>	-0.444	O <sub>12</sub>	-0.474	O <sub>12</sub>	-0.435	O <sub>1</sub>	-0.429	O <sub>12</sub>	-0.306
-	-	-	-	O <sub>1</sub>	-0.362	O <sub>1</sub>	-0.431	O <sub>1</sub>	-0.363	-	-	O <sub>1</sub>	-0.158

<sup>a</sup>Different atoms involved in ICT. <sup>b</sup>Mulliken charges on different atoms.

**Table 6.** Molecular Orbitals Properties of Coumarins

Molecule	Energy (eV)		
	HOMO	LUMO	$\Delta E^a$
C-1	-3.782	-0.816	2.966
C-2	-5.888	-1.742	4.146
C-3	-6.504	-2.176	4.328
C-4	-6.150	-1.742	4.408
C-5	-6.394	-1.986	4.408
C-6	-6.258	-2.041	4.217
C-7	-5.986	-1.960	4.026

<sup>a</sup> $\Delta E = E_{LUMO} - E_{HOMO}$ .

the coumarins, however, C-7 stimulates ICT more than coumarins C-2 to C-6 as evident from the lowest  $\Delta E$  value of 4.026 eV. This can be explained on the basis of the substituent effect as the R<sub>3</sub> position of coumarins *i.e.* 7<sup>th</sup> position increases the conjugation in coumarins which in turn proliferates the mobility of  $\pi$  electrons providing more polarizable characteristics to the molecule and a favorable ICT process [9]. As can be visualized from the spatial overlap of the HOMO and LUMO, the S<sub>0</sub> → S<sub>1</sub> electronic transition designated this charge transfer process as intense one.

The ICT route was also supported by Mulliken atomic charges acquired from the DFT/BL3YP calculations. The Mulliken charges for the selected atoms participating in the

typical ICT process are listed in Table 5. The hydrogen atom connected to the R<sub>3</sub> group has the most positive charge (in the range 0.392-0.156) while the carbonyl oxygen atom of the pyranone ring has the most negative charge (-0.306 to -0.474), thereby complementing them as electron donor (R<sub>3</sub> = -OH, -NH<sub>2</sub>, -OCH<sub>3</sub>, -OC<sub>2</sub>H<sub>5</sub>) and electron acceptor

(-C=O) sites supporting the ICT process. Thus, the charge transfer in coumarins occurs from the R<sub>3</sub> group of benzene to the carbonyl group of the pyranone ring.

ESP surfaces can also be used to understand the solute-solvent interactions as well as different interaction sites within coumarins (Fig. 6) [47,48]. Distinct colors distinguish

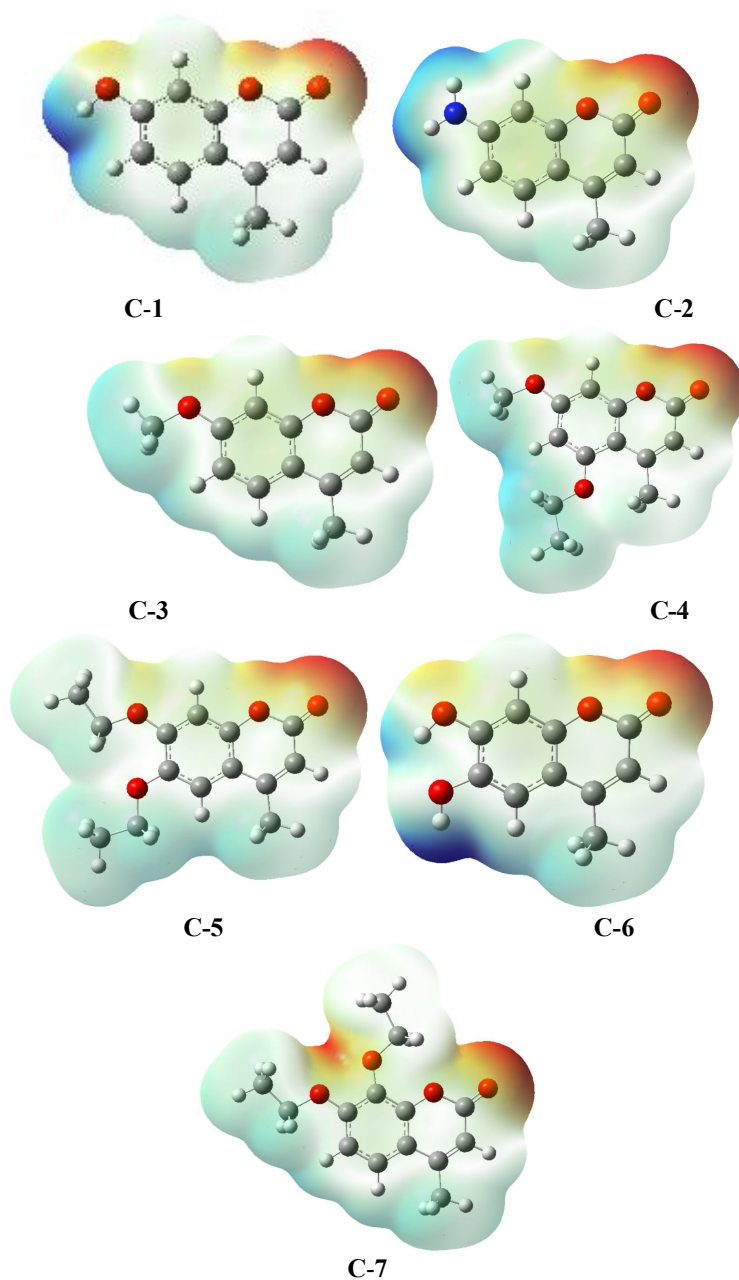


**Fig. 6.** MEP surfaces for different coumarins with isosurface value of 0.0004.

the different ESP areas (positive, negative, or neutral) on a surface. The color red denotes the most negative ESP zone, the color blue denotes the most positive ESP zone, and the color green denotes regions with zero potential. The oxygen atoms and carbonyl group of the pyranone ring as well as the oxygen atoms of the R<sub>1</sub>-R<sub>4</sub> groups have a negative ESP zone and can absorb hydrogen from hydrogen bond donor solvents, as shown in Fig. 6.

The hydrogen atoms in both rings, on the other hand, have a positive ESP and can be transferred to hydrogen-deficient solvents. Depending on the solvent available for interaction, coumarins can operate as a hydrogen donor or an acceptor. On the basis of the Mulliken charges of the individual atoms, the hydrogen atoms connected to the R<sub>3</sub> group and the carbonyl oxygen atom of the pyranone ring are labeled as electrophilic and nucleophilic sites, respectively (Table 5). The solvent dependence of coumarins can further be represented by dielectric continuum models where solvation takes into account the solvent alignment.

**Solvation of coumarins.** Dielectric continuum models are popular for modeling solvent effects in quantum chemical calculations. Although the solvent can always be explicitly reintroduced as an ambient skin for the first solvation shells, the use of continuum models requires that there be no significant specific interactions between the solvent and the solute molecules. Inside the cavity, the dielectric constant is 1, outside, it has a fixed value (equal to the dielectric constant of the solvent). The IEFPCM solvation model, which employs a modified dielectric boundary condition that combines dielectric exactness with abridged charge sensitivity, was used to solvate the molecules [49].

Intermolecular interactions are the summation of many components, including cavity formation energy ( $E_{\text{cav}}$ ), electrostatic energy ( $E_{\text{el}}$ ), Polarized solute-solvent interaction energy ( $\Delta E_{\text{PSS}}$ ), and solute-solvent repulsion energy ( $E_{\text{rep}}$ ). The interaction between the dielectric medium and the charge distribution of the solute provides the electrostatic component of the solvation free energy ( $\Delta G_{\text{sol}}$ ) in continuous models, which is the largest contribution for polar and charged solutes.  $\Delta G_{\text{sol}}$  corresponds to the process of transferring the solute molecule from a fixed position in the gas phase to a fixed position in the solution at constant temperature, pressure, and chemical composition [50,51]. In the case of the continuum dielectric model,  $\Delta G_{\text{sol}}$  can be

regarded as the sum of several components of which the electrostatic interactions (hydrogen bonding, dipole-dipole interactions, and others), the cavitation, and the dispersion contributions are the most relevant.  $\Delta G_{\text{sol}}$  can be defined as:

$$\Delta G_{\text{sol}} = \Delta G_{\text{cav}} + \Delta G_{\text{PSS}} + \Delta G_{\text{dis}} \quad (7)$$

$E_{\text{cav}}$  approximates the solvent accessible surface area to introduce a solute in the cavity of the solvent and is defined as the work involved in creating the appropriate cavity inside the solution in the absence of solute-solvent interactions. The dispersion energy ( $E_{\text{dis}}$ ) is thought to be the most isotropic component of a van der Waals interaction. These are temporary induced attractive interactions that occur when two molecules are almost touching. Although dispersion energy has little effect on the equilibrium orientation of the cluster, it does contribute significantly to the energy of hydrogen bonding. It plays a crucial role as the size of the system increases [52].

Different solvation parameters like  $E_{\text{cav}}$ ,  $E_{\text{dis}}$ ,  $E_{\text{rep}}$ ,  $E_{\text{PSS}}$ , total non-electrostatic energy ( $E_{\text{non-el}}$ ), and solvation free energy ( $\Delta G_{\text{sol}}$ ) of the coumarins were calculated computationally using TD-DFT approach (Table 7). According to theoretically derived  $E_{\text{cav}}$  values, coumarins have larger cavitation energy in the presence of water than benzene and ethanol. Because coumarins are polar moieties, they penetrate the cavities in the solvents, increasing the surface area and causing the coumarins to have a larger  $E_{\text{cav}}$ . Furthermore,  $E_{\text{cav}}$  values for tri-substituted coumarins are higher than those for di-substituted coumarins because the former has a larger surface area than the latter. C-6, on the other hand, has a lower  $E_{\text{cav}}$  value than its equivalents because it forms hydrogen bonds with water molecules.

$E_{\text{dis}}$  values of coumarins show that the dispersion energy increases in the following order: water < benzene < ethanol.  $E_{\text{dis}}$  is proportional to the size of a molecule; as the size of a molecule increases, so does  $E_{\text{dis}}$ . Furthermore, when the mass of a non-polar molecule is large enough, its dispersion forces can be stronger than the dipole-dipole forces in a lighter polar molecule [53,54]. Despite the fact that benzene has a larger size than ethanol and water, it must have higher dispersion energy, but it has a lower  $E_{\text{dis}}$  value than ethanol. The reason for this is that benzene is aromatic, and dispersion energy contributes to aromatic  $\pi$ -stacking interactions, which in turn

take their share of dispersion energy, resulting in a decrease in dispersion energy. The  $E_{\text{non-el}}$  of coumarins also follows the same order: ethanol < benzene < water as that of  $E_{\text{dis}}$ .

The electrostatic and polarization components of the interaction energy are the most prominent interaction terms in ethanol and water. These contributions account for specific interactions, such as the ubiquitous hydrogen bonds of these solvents with coumarins, which are generally stronger than ordinary dispersion forces. When ethanol and water are compared, the former has more dispersion energy than the latter because ethanol is a larger molecule than water, increasing the van der Waals dispersion forces.

When it comes to repulsion energy, coumarins have lower  $E_{\text{rep}}$  values for ethanol and water than benzene. Because coumarins are polar in nature, they can interact strongly with the polar solvents: water and ethanol, according to the rule "like dissolves like". Benzene is non-polar due to its large hydrocarbon part, its interactions with coumarins are too weak. Solvent-solute interactions are significant to physical organic chemistry and have been studied for over a century. The polarized solute-solvent interactions ( $E_{\text{PSS}}$ ) follow a pattern in the following order: benzene < ethanol < water. When polar molecules are solvated by polar solvents as previously discussed, coumarins are polar they are solvated more by the polar solvents ethanol and water than non-polar solvent benzene. As a result, the specific interactions of coumarins with water are much more stabilized than those of ethanol and benzene, thus,  $E_{\text{PSS}}$  for water is greater than that of ethanol and benzene.

Coumarins showed noticeable structural changes when solvated by different solvents, as evidenced by their solvation energies in benzene, ethanol, and water (Table 7). C-1 has solvation energies (in kcal mol<sup>-1</sup>) of -3.78, -15.88, and -12.53, in benzene, ethanol, and water. Considering the solvation energy difference of C-1 between highly polar solvent (water) and least polar solvent (benzene), we got a value of -8.75 kcal mol<sup>-1</sup>. Also, the difference in  $\Delta G_{\text{sol}}$  value of C-1 between ethanol and benzene gave a value of -12.10 kcal mol<sup>-1</sup>. Other coumarins, C2-C7 also bear a similar behavior. The difference in solvent energies justify the structural variations in coumarins C-1 to C-7 as the substituents differ from polar -OH, -NH<sub>2</sub> groups to non-polar -OCH<sub>3</sub> and -OC<sub>2</sub>H<sub>5</sub> groups in a range of solvents varying from non-polar benzene to most polar solvent (water)

justifying solute-solvent interactions.

**Oscillator strength and excitation spectra.** The oscillating transition dipole is also related to the oscillator strength ( $f$  value) due to the redistribution of electron density from HOMO-LUMO. The  $f$  values obtained theoretically in the gaseous phase, benzene, ethanol, and water are tabulated in Table 8. On comparing  $f$  values of coumarins in the gaseous phase to the corresponding ones in the solution, it is revealed that the  $f$  values in the gaseous phase are lower than the solution phase as solvent facilitates an increase in oscillator strength for any given transition [55,56]. Additionally, the obtained  $f$  values are found to be less than 1, implying that the intensity of these bands is due to a single optical transition. The  $f$  values of an electronic transition of coumarins in a sequence of solvents increase when the solvent polarity changes from benzene to water because all van der Waal's interactions between solute and solvent including dispersion interaction are operational in the perturbation of the oscillator strength. However, an exception is observed for C-4 and C-5, which have a high  $f$  value in benzene as these molecules are less polar than other coumarins, here only the dispersion interaction terms exist.

The absorption spectra of coumarins C-1 to C-7 were considered theoretically using the compounds optimal ground state geometries. For the purpose of validating the computational study, the same conditions were employed with different functional as in the experimental values. The excitation spectra were determined using TD-DFT calculations incorporating the IEFPCM solvation model and the corresponding wavelengths are presented in Tables 8 and S4. The experimentally measured  $\lambda_{\text{max}}$  values matched appreciably with the theoretically determined  $\lambda_{\text{max}}$  values (Table 8).

The results of calculations (Tables 7, 8, and S4) predicted that the lowest energy absorption band of coumarins in the range 3.338-4.084 eV ( $\lambda_{\text{max}} = 336.37$ - $303.52$  nm) arises from a single electronic transition from HOMO to LUMO orbital and is quite intense ( $f$  values in range = 0.143-0.394) for longer wavelengths bands in all the solvents. This confirms the strong charge transfer characteristics of coumarins and the corresponding transition to be the intense one as revealed by their highly fluorescent nature. The band gap values were almost similar to the  $\Delta E$  values obtained from their respective HOMO and LUMO orbital plots (Table 6).

**Table 7.** Theoretical Calculated Excitation Energy<sup>a</sup> and other Solvent Associated Energies of Coumarins

Molecule	C-1				C-2			
	Gaseous	Benzene	Ethanol	Water	Gaseous	Benzene	Ethanol	Water
$E_{\text{ext}}$ (eV)	3.997	3.765	4.077	4.070	3.857	3.714	3.558	3.545
$E_{\text{Cav}}$ (Kcal mol <sup>-1</sup> )	-	20.06	18.29	25.19	-	20.37	18.58	25.62
$E_{\text{Disper}}$ (Kcal mol <sup>-1</sup> )	-	-16.61	-15.35	-17.41	-	-16.99	-15.71	-17.81
$E_{\text{Repu}}$ (Kcal mol <sup>-1</sup> )	-	1.75	1.04	1.24	-	1.76	1.04	1.24
$E_{\text{non-el}}$ (Kcal mol <sup>-1</sup> )	-	5.2	3.98	9.03	-	5.13	3.91	9.06
$E_{\text{PSS}}$ (Kcal mol <sup>-1</sup> )	-	-7.23	-18.82	-20.31	-	-6.6	-16.74	-17.94
$\Delta G_{\text{sol}}$ (Kcal mol <sup>-1</sup> )	-	-3.78	-15.88	-12.53	-	-3.22	-13.87	-10.13
Molecule	C-3				C-4			
	Gaseous	Benzene	Ethanol	Water	Gaseous	Benzene	Ethanol	Water
$E_{\text{ext}}$ (eV)	3.432	4.025	3.954	3.953	3.9973	3.854	3.768	3.751
$E_{\text{Cav}}$ (Kcal mol <sup>-1</sup> )	-	22.48	20.52	27.71	-	27.20	24.83	36.21
$E_{\text{Disper}}$ (Kcal mol <sup>-1</sup> )	-	-17.13	-15.83	-17.86	-	-19.65	-18.15	-21.81
$E_{\text{Repu}}$ (Kcal mol <sup>-1</sup> )	-	-5.53	0.83	0.97	-	1.50	0.86	1.10
$E_{\text{non-el}}$ (Kcal mol <sup>-1</sup> )	-	6.80	5.52	10.82	-	9.05	7.54	15.5
$E_{\text{PSS}}$ (Kcal mol <sup>-1</sup> )	-	-5.53	-14.4	-15.24	-	-5.57	-14.06	-15.51
$\Delta G_{\text{sol}}$ (Kcal mol <sup>-1</sup> )	-	-0.18	-9.71	-5.39	-	1.98	-7.38	-1.11
Molecule	C-5				C-6			
	Gaseous	Benzene	Ethanol	Water	Gaseous	Benzene	Ethanol	Water
$E_{\text{ext}}$ (eV)	3.893	3.822	3.802	3.801	3.487	3.334	3.724	3.686
$E_{\text{Cav}}$ (Kcal mol <sup>-1</sup> )	-	27.05	24.70	34.26	-	20.99	19.47	26.31
$E_{\text{Disper}}$ (Kcal mol <sup>-1</sup> )	-	-20.22	-18.69	-21.16	-	-17.55	-16.2	-18.4
$E_{\text{Repu}}$ (Kcal mol <sup>-1</sup> )	-	1.53	0.88	1.05	-	1.85	1.1	1.32
$E_{\text{non-el}}$ (Kcal mol <sup>-1</sup> )	-	8.36	6.89	14.15	-	5.290	4.37	9.22
$E_{\text{PSS}}$ (Kcal mol <sup>-1</sup> )	-	-5.28	-13.39	-14.56	-	-8.39	-23.44	-24.23
$\Delta G_{\text{sol}}$ (Kcal mol <sup>-1</sup> )	-	1.55	-7.38	-1.46	-	-4.95	-20.17	-16.32

<sup>a</sup>Calculated using TD-DFT approach using B3LYP with 6-311++G(d,p) basis set.

$f$  values are found to be zero for C-1 ( $f = 0.00$ ) and C-6 ( $f = 0.00$ ) in the case of non-polar solvent benzene as these are disallowed transitions either a weakly allowed transition

due to the change of spin state in the atom [57]. The  $f$  values corresponding to smaller wavelength bands are either zero or very low as these transitions are masked under the envelope

**Table 8.** Comparison of Experimental and Theoretical Absorption Band Maxima Values of Coumarins in Benzene, Ethanol, and Water

Solvent Molecule	$\lambda$ (in benzene)		$\lambda$ (in ethanol)		$\lambda$ (in water)	
	exp <sup>a</sup>	Th <sup>b</sup>	exp	Th	exp	Th
C-1	285,	-,	295,	280.00 (0.006) <sup>c</sup> ,	296,	286.12 (0.005),
	320	329.28 (0.000)	324	304.14 (0.304)	322	313.62 (0.298)
C-2	300,	285.55 (0.082),	307,	306.12 (0.000),	310,	305.45 (0.016),
	345	333.85 (0.345)	354	348.45 (0.296)	342	349.72 (0.290)
C-3	285,	-,	287,	286.11 (0.018),	290,	286.11 (0.023),
	319	314.65 (0.000)	320	313.60 (0.324)	321	313.61 (0.394)
C-4	-,	295.35 (0.134),	235,	249.73 (0.000),	240,	248.13 (0.000),
	319	321.74 (0.366)	320	329.11 (0.295)	323	330.58 (0.299)
C-5	-,	293.59 (0.072),	232,	-,	240,	261.86 (0.008),
	320	324.40 (0.268)	321	326.07 (0.241)	323	326.18 (0.236)
C-6	305,	304.28 (0.143),	310,	311.14 (0.018),	312,	307.53 (0.006),
	348	335.00 (0.304)	346	355.50 (0.286)	348	336.37 (0.257)
C-7	-,	303.52 (0.148),	254,	272.30 (0.001),	255,	271.33 (0.001),
	315	330.34 (0.158)	318	328.28 (0.164)	320	327.22 (0.166)

<sup>a</sup>Experimentally determined absorption band maxima. <sup>b</sup>theoretically calculated absorption band maxima. <sup>c</sup> $f$  values are given in parenthesis.

of the intense transitions or probably not detected in the experimental observation. This data also supports the idea that ICT is more effective in polar solvents than non-polar solvents (Table S5).

### Dipole Moments of Coumarins

Non-specific solvent effects bring solvatochromic shifts relating the transition energy of the molecules as a difference between wavenumbers of absorption and fluorescence bands maxima correlating them with the dielectric constant ( $\epsilon$ ) and refractive index ( $n$ ) of the solvents, which estimates the dipole moment of a solute. The spectral shifts: ( $\bar{\nu}_a - \bar{\nu}_f$ ) and ( $\bar{\nu}_a + \bar{\nu}_f$ ) for coumarins were derived from their absorption and fluorescence spectrum data in different solvents to

evaluate dipole moments. The spectral shifts were shown against the variables  $f(\epsilon, n)$  and  $E_T^N$ , while ( $\bar{\nu}_a + \bar{\nu}_f$ ) were plotted against the variable  $\rho(\epsilon, n)$  (Fig. 7). The best-fit plots revealed a strong linear relationship between spectral changes and polarity parameters. Table 9 lists the theoretically calculated parameters:  $a$ ,  $\mu_g$ , and  $\mu_o/\mu_g$  (= ratio) derived from the slopes  $m_1$  and  $m_2$  (Eqs. (1) and (2)), and  $\Delta\mu$  (= change) acquired from slope  $m_3$  (Eq. (6)) as well as  $\mu_e$  derived using  $\mu_g$ . For coumarins, high values of  $\Delta\mu$ ,  $\mu_o/\mu_g$ , and unusually exaggerated  $\mu_e$  values confirm increase in conjugation and charge mobility of coumarins in their excited state.

A large ICT *via* electron density transfer from the benzene ring to the pyranone ring (Fig. 5) results in large



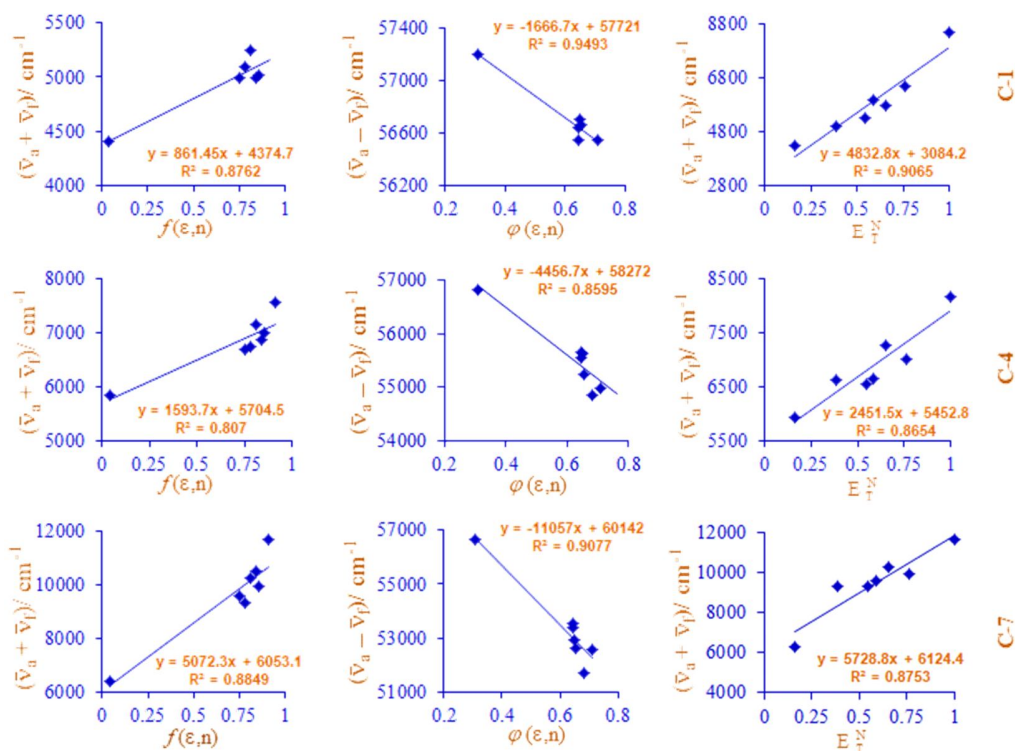


Fig. 7. Plots of spectral shifts as a function of various polarity parameters for C-1, C-4, and C-7.

Table 9. Dipole moments ( $\mu_e/\mu_g$  and  $\Delta\mu$ ) Calculated from Solvatochromic Models

Molecule	Cavity radius $a^a$ (Å)	$\mu_g^a$ (D)	Kawski <i>et al.</i>				Ravi <i>et al.</i>		
			Slopes ( $\text{cm}^{-1}$ )		Dipole moment (D)		Slope ( $\text{cm}^{-1}$ )	Dipole moment (D)	
			$m_1^b$	$-m_2^b$	$\mu_e/\mu_g^c$	$\mu_e^d$	$m_3^e$	$\Delta\mu^f$	$\mu_e^d$
C-1	3.184	7.357	861	1667	3.136	23.075	4833	2.165	9.522
C-2	3.238	7.146	10340	4758	2.705	19.328	2857	1.707	8.853
C-3	3.786	7.436	865	2149	2.347	17.455	943	1.240	8.676
C-4	4.248	6.233	1594	4457	2.114	13.174	2452	2.377	8.610
C-5	3.786	7.863	854	4086	1.528	12.018	903	1.214	9.077
C-6	3.074	7.971	512	3368	1.359	10.829	428	0.611	8.582
C-7	4.246	5.899	5072	11057	2.695	16.568	5822	3.660	9.779

<sup>a</sup>Theoretically calculated parameters. <sup>b</sup>Calculated from the plots of  $(\bar{\nu}_a - \bar{\nu}_f)$  vs.  $f(\epsilon, n)$  and  $(\bar{\nu}_a + \bar{\nu}_f)$  vs.  $\varphi(\epsilon, n)$  (Eqs. (1) and (2)).

<sup>c</sup>Calculated using ratio of  $m_1$  and  $m_2$ ,  $\frac{\mu_e}{\mu_g} = \left( \frac{m_1 + m_2}{m_2 - m_1} \right)$  (Eqs. (3a) and (3b)). <sup>d</sup>Calculated using  $\mu_g$ . <sup>e</sup>Calculated from the plots of  $\bar{\nu}_a - \bar{\nu}_f$

vs.  $E_T^N$  (Eq. (5)). <sup>f</sup>Calculated using  $m_3$  (Eq. (6)).



dipole moments of coumarins in their excited state rendering its fluorescence emission sensitive to the environment and solvent polarity. The di-substituted coumarins C-1, C-2, and C-3 have substantial dipole moments due to the presence of highly polar functional groups in the 7<sup>th</sup> position, which allow charge density transfer. Due to the substantial charge separation in the excited states of coumarins, the experimentally calculated  $\mu_e$  values of these molecules demonstrate an increase in the excited state dipole moment. However, because charge transfer in these molecules is impeded by the presence of substituents at two consecutive sites, the dipole moments of tri-substituted coumarins C-5 and C-6 are significantly lower than those of other coumarins. Because the second ethoxy group in C-7 is positioned axially, the charge transfer mechanism is not hampered, and has a substantially greater dipole moment than its analogues C-5 and C-6 and is comparable to di- substituted coumarins.

The molecular orbital graphs HOMO-1, HOMO, LUMO, and LUMO+1 also validate the ICT route. The Mulliken charges also established the presence of nucleophilic and electrophilic centers in the coumarins and complemented the suggested ICT mechanism. The ICT is found to be intensified in polar solvents as visualized by noting the theoretical dipole moments of coumarins in different mediums using DFT studies (Table S5). Coumarins experience a high dipole moment in water than ethanol and benzene facilitating the ICT process more in polar solvents.

## CONCLUSIONS

The photophysical characteristics of di- and tri-substituted coumarins in various solvents have been examined. The absorption maximum of coumarins was slightly affected by solvent polarity. Surprisingly, coumarins displayed distinct charge redistribution in their excited states, resulting in substantial Stokes shifts in their excited state, implying that these molecules have an ICT characteristic. When compared to di-substituted coumarins, the tri-substituted coumarins have higher bathochromic shifts. However, steric crowding caused by substituents appearing in consecutive locations disrupts charge density transfer, resulting in a decrease in the dipole moments of tri-substituted coumarins. Different possible solute-solvent interactions were also anticipated based on Mulliken atomic

charges, FMO graphs, and ESP maps analysis. The ESP maps and the Mulliken atomic charges categorized the R<sub>3</sub> group on the benzene ring and carbonyl group as the electrophilic and nucleophilic sites, respectively. The IEFPCM solvation model successfully explained the solvation of coumarins and reveals that ICT is intensified in the polar solvents. The theoretical values are found to be in good agreement with experimental values. The findings revealed that increasing the polarity of the solvent contributes to the occurrence of excited state dynamic processes.

## ACKNOWLEDGEMENTS

The authors are thankful to the University Grants Commission (UGC), New Delhi for the funding.

## REFERENCES

- [1] Costa, T. M.; Tavares, L. B. B., de Oliveira, Fungi as a Source of natural coumarins production. *Appl. Microbiol. Biotechnol.* **2016**, *100*, 6571-6584, DOI: 10.1039/js8682100053.
- [2] Khan, I. A.; Kulkarni, M. V.; Sun, C. M., One pot synthesis of oxygenated tri-heterocycles as anti-microbial agents. *Eur. J. Med. Chem.* **2005**, *40*(11), 1168-1172, DOI: 10.1016/j.ejmech.2005.05.007.
- [3] Neyts, J.; Clercq, E. D.; Singha, R.; Chang, Y. H.; Das, A. R.; Chakraborty, S. K.; Hwu, J. R., Structure-activity relationship of new anti-Hepatitis C virus agents: Heterobicycle-coumarin conjugates. *J. Med. Chem.* **2009**, *52*(5), 1486-1490, DOI: 10.1021/jm801240d.
- [4] Liu, X.; Cole, J. M.; Waddell, P. G.; Lin, T. C.; Radia, J.; Zeidler A., Molecular origins of optoelectronic properties in coumarin dyes: Toward designer solar cell and laser applications. *J. Phys. Chem. A* **2012**, *116*(1), 727-737, DOI: 10.1021/jp209925y.
- [5] Mandlik, V.; Patil, S.; Bopanna, R.; Basu, S.; Singh, S., Biological activity of coumarin derivatives as anti-leishmanial agents. *PLoS One* **2016**, *11*(10), e0164585, DOI: 10.1371/journal.pone.0164585.
- [6] Cao, D.; Liu, Z.; Verwilt, P.; Koo, S.; Jangili, P.; Kim, J. S.; Lin, W., Coumarin-based small-molecule fluorescent chemosensors. *Chem. Rev.* **2019**, *119*(18),

- 10403-10519, DOI: 10.1021/acs.chemrev.9b00145.
- [7] Yamaji, M.; Hakoda, Y.; Okamoto, H.; Tanid., F., Photochemical synthesis and photophysical properties of coumarins bearing extended polyaromatic rings studied by emission and transient absorption measurements. *Photochem. Photobiol. Sci.* **2017**, *16*, 555-563, DOI: 10.1039/C6PP00399K.
- [8] Han, J.; Cao, B.; Li, Y.; Zhou, Q.; Sun, C.; Li, B.; Yin, H.; Shi, Y., The role played by solvent polarity in regulating the competitive mechanism between ESIP and TICT of coumarin (E-8-((4-dimethylamino-phenylimino)-methyl)-7-hydroxy-4-methyl-2H-chromen-2-one). *Spectrochim. Acta A* **2020**, *231*, 118086, DOI: 10.1016/j.saa.2020.118086.
- [9] Bourbon, P.; Peng, Q.; Ferraudi, G.; Stauffacher, C.; Wiest, O.; Helquist, P., Synthesis, photophysical, photochemical, and computational studies of coumarin-labeled nicotinamide derivatives. *J. Org. Chem.* **2012**, *77*, 2756-2762, DOI: 10.1021/jo2025527.
- [10] Raghavendra, U. P.; Basanagouda, M.; Melavanki, R. M.; Fattepur, R. H.; Thipperudrappa, J., Solvatochromic studies of biologically active iodinated 4-aryloxymethyl coumarins and estimation of dipole moments. *J. Mol. Liq.* **2015**, *202*, 9-16, DOI: 10.1016/j.molliq.2014.12.003.
- [11] Cartwright, S. J., Solvatochromic dyes detect the presence of homeopathic potencies, *Homeopathy* **2016**, *105*, 55-65, DOI: 10.1016/j.homp.2015.08.002.
- [12] Gonciarz, A.; Zuber, M.; Zwoździak, J., Spectrochemical properties and solvatochromism of tetradentate schiff base complex with nickel: calculations and experiments. *Chem. Open* **2018**, *7*(9), 677-687, DOI: 10.1002/open.201800100.
- [13] Jana, P.; Siva, A.; Soppina, V.; Kanvah, S., Live-cell imaging of lipid droplets using solvatochromic coumarin derivatives. *Org. Biomol. Chem.* **2020**, *18*, 5608-5616, DOI: 10.1039/D0OB01277G.
- [14] Giri, R., Fluorescence quenching of coumarins by halide ions. *Spectrochim. Acta A* **2004**, *60*(4), 757-763, DOI: 10.1016/S1386-1425(03)00287-7.
- [15] Liu, X.; Cole, J. M.; Low, K. S., The electronic absorption spectra of some coumarins. A molecular orbital treatment. *J. Phys. Chem. C* **2013**, *117*(28), 14731-14741, DOI: 10.1021/jp310397z.
- [16] Holubekova, A.; Mach, P.; Urban, J., Spectral properties of coumarin derivatives in various environments. *Cent. Eur. J. Chem.* **2013**, *11*, 492-501, DOI: 10.2478/s11532-012-0185-0.
- [17] Tasiór, M.; Kim, D.; Singha, S.; Krzeszewski, M.; Ahn, K. H.; Gryko, D. T.,  $\pi$ -Expanded coumarins: synthesis, optical properties and applications. *J. Mater. Chem. C* **2015**, *3*(7), 1421-1446, DOI: 10.1039/C4TC02665A.
- [18] Lapina, V. A.; Pavich, T. A.; Pershukevich, P. P.; Trofimov, A. V.; Trofimova, N. N.; Tsaplev, Y. B.; Zak, P. P., Exploring the utility of coumarins-based luminescent spectra converters. *J. Phys. Org. Chem.* **2017**, *30*, e3731, DOI: 10.1002/poc.3731.
- [19] Kolbus, A.; Danel, A.; Grabka, D.; Kucharek, M.; Szary, K., Spectral properties of highly emissive derivative of coumarin with N,N-diethylamino, nitrile and thiophenecarbonyl moieties in water-methanol mixture. *J. Fluoresc.* **2019**, *29*, 1393-1399, DOI: 10.1007/s10895-019-02446-5.
- [20] Petersilka, M.; Gross, E. K. U.; Burke, K., Excitation energies from time-dependent density functional theory using exact and approximate potentials. *Int. J. Quantum Chem.* **2000**, *80*, 534-554, DOI: 10.1002/1097-461X(2000)80:4/5<534::AID-QUA3>3.0.CO;2-V.
- [21] Gonçalves, P. F. B.; Stassen, H., Calculation of the free energy of solvation from molecular dynamics simulations. *Pure Appl. Chem.* **2004**, *76*(1), 231-240, DOI: 10.1351/pac200476010231.
- [22] Riley, K. E.; Vondrášek, J.; Hobza, P., Performance of the DFT-D method, paired with the PCM implicit solvation model, for the computation of interaction energies of solvated complexes of biological interest. *Phys. Chem. Chem. Phys.* **2007**, *9*, 5555-5560, DOI: 10.1039/B708089A.
- [23] Giri, R.; Rathi, S. S.; Machwe, M. K.; Murti, V. V. S., Effect of substituents on the fluorescence and absorption spectra of coumarins. *Spectrochimica Acta A* **1988**, *44*(8), 805-807, DOI: 10.1016/0584-8539(88)80146-6.
- [24] GaussView 3.0, SemiChem, Inc., USA, 2000-2003.
- [25] Tomasi, J.; Mennucci, B.; Cammi, R., Quantum mechanical continuum solvation models, *Chem. Rev.* **2005**, *105*(8), 2999-3094, DOI: 10.1021/cr9904009.
- [26] Payal, R.; Saroj, M. K.; Sharma, N.; Rastogi, R. C.,

- Photophysical behavior of some thymol based schiff bases using absorption and fluorescence spectroscopy. *J. Lumin.* **2018**, *198*, 92-102, DOI: 10.1016/j.jlumin.2018.02.007.
- [27] Kawski, A., On the estimation of excited-state dipole moments from solvatochromic shifts of absorption and fluorescence spectra. *Z. Naturforsch.* **2002**, *57a(5)*, 255-262, DOI: 10.1515/zna-2002-0509.
- [28] Bilot, L.; Kawski, A., Theory of the effect of solvents on the electron spectra of molecules. *Z. Naturforsch.* **1962**, *17a*, 621-627.
- [29] Kawski, A.; Kukliński, B.; Bojarski, P., Thermochromic absorption, fluorescence band shifts and dipole moments of badan and acrylodan. *Z. Naturforsch.* **2002**, *57a(8)*, 716-722, DOI: 10.1515/zna-2002-0812.
- [30] Kawski, A.; Bojarski, P.; Kukliński, B., Excitation wavelength dependence of acrylodan fluorescence spectra in some polar solvents. *Z. Naturforsch.* **2002**, *57a(9-10)*, 94-97, DOI: 10.1515/zna-2002-9-1015.
- [31] Kawski, A.; Kukliński, B.; Bojarski, P., Thermochromic shifts of absorption and fluorescence spectra and excited state dipole moment of prodan. *Z. Naturforsch.* **2000**, *55a(5)*, 550-554, DOI: 10.1515/zna-2000-0512.
- [32] Kawski, A.; Kukliński, B.; Bojarski, P., Ground and excited state dipole moments of badan and acrylodan determined from solvatochromic shifts of absorption and fluorescence spectra. *Z. Naturforsch.* **2001**, *56a(5)*, 407-411, DOI: 10.1515/zna-2001-0510.
- [33] Onsager, L., Electric moments of molecules in liquids. *J. Am. Chem. Soc.* **1936**, *58*, 1486-1493, DOI: 10.1021/ja01299a050.
- [34] Ravi, M.; Samanta, A. T.; Radhakrishnan, P., Excited state dipole moments from an efficient analysis of solvatochromic stokes shift data. *J. Phys. Chem.* **1994**, *98(37)*, 9133-9136, DOI: 10.1021/j100088a007.
- [35] Reichardt, C.; Che, D.; Heckenkemper, G.; Schäfer, G., Syntheses and UV-Vis-spectroscopic properties of hydrophilic 2-, 3-, and 4-pyridyl-substituted solvatochromic and halochromic pyridinium n-phenolate betaine dyes as new empirical solvent polarity indicators. *Eur. J. Org. Chem.* **2001**, *12*, 2343-2361, DOI: 10.1002/1099-0690(200106)2001:12<2343::AID-EJOC2343>3.0.CO;2-I.
- [36] Reichardt, C., Pyridinium N-phenolate betaine dyes as empirical indicators of solvent polarity: some new findings. *Pure Appl. Chem.* **2004**, *76(10)*, 1903-1919, DOI: 10.1351/pac200476101903.
- [37] Reichardt, C., Pyridinium-N-phenolate betaine dyes as empirical indicators of solvent polarity: some new findings. *Pure Appl. Chem.* **2008**, *80(7)*, 1415-1432, DOI: 10.1351/pac200880071415.
- [38] Reichardt, C.; Welton, T., Solvents and solvent effects in organic chemistry. Wiley-VCH Verlag GmbH & Co. KGaA: **2010**, p. 425-508.
- [39] Lippert, E. Z., Dipole moment and electronic structure of excited molecules. *Z. Naturforsch.* **1955**, *10a*, 541-545.
- [40] Giri, R.; Tiwari, Y., Influence of solvents and temperature on the photophysical characteristics of flavanones. *Indian J. Pure Appl. Phys.* **2003**, *41*, 530-537.
- [41] Giri, R., On the fluorescence quenching of substituted coumarins. *J. Pure Appl. Sci. Tech.* **2015**, *5(2)*, 22-26.
- [42] Veselinović, J. B.; Veselinović, A. M.; Vitnik, Ž. J.; Vitnik, V. D.; Nikolić, G. M., Antioxidant properties of selected 4-phenyl hydroxycoumarins: integrated in vitro and computational studies. *Chem. Biol. Interact.* **2014**, *214*, 49-56, DOI: 10.1016/j.cbi.2014.02.010.
- [43] Latha, B.; Kumaresan, P.; Nithiyantham, S.; Sampathkumar, K., Spectroscopic, HOMO-LUMO and NLO studies of tetra fluoro phthalate doped coumarin crystals using DFT method. *J. Mol. Struct.* **2017**, *1142*, 255-260, DOI: 10.1016/j.molstruc.2017.04.078.
- [44] Irfan, M.; Iqbal, J.; Eliasson, B.; Ayub, K.; Rana, U. A.; Khan, S. U., Benchmark study of UV-Vis spectra of coumarin derivatives by computational approach. *J. Mol. Struct.* **2017**, *1130*, 603-616, DOI: 10.1016/j.molstruc.2016.11.026.
- [45] Orbulescu, J.; Kele, P.; Kotschy, A.; Leblanc, R. M., Synthesis and spectroscopy of coumarin derivatives for saxitoxin detection. *J. Mater. Chem.* **2005**, *15*, 3084-3088, DOI: 10.1039/B501510C.
- [46] SambathKumar, K.; Nithiyantham, S., Synthesis, characterization and theoretical properties of coumarin NLO single crystal by DFT method, *J. Mater. Sci.*

- Mater. Electron.* **2017**, *28*, 6529-6543, DOI: 10.1007/s10854-017-6342-7.
- [47] Rathi, P. C.; Ludlow, R. F.; Verdonk, M. L., Practical high-quality electrostatic potential surfaces for drug discovery using a graph-convolutional deep neural network. *J. Med. Chem.* **2020**, *63*(16), 8778-8790, DOI: 10.1021/acs.jmedchem.9b01129.
- [48] Saroj, M. K.; Payal, R.; Jain, S. K.; Rastogi, R. C., Study of prototropic reactions of indole chalcone derivatives in ground and excited states using absorption and fluorescence spectroscopy. *J. Mol. Liq.* **2020**, *302*, 112164, DOI: 10.1016/j.molliq.2019.112164.
- [49] Klamt, A.; Moya, C.; Palomar, J., A comprehensive comparison of the IEFPCM and SS(V)PE continuum solvation methods with the COSMO approach. *J. Chem. Theory Comput.* **2015**, *11*(9), 4220-4225, DOI: 10.1021/acs.jctc.5b00601.
- [50] Scherlis, D. A., Unified electrostatic and cavitation model for first-principles molecular dynamics in solution. *J. Chem. Phys.*, **2006**, *124*(7), 074103, DOI: 10.1063/1.2168456.
- [51] Gonçalves, P. F. B.; Stassen, H., Calculation of the free energy of solvation from molecular dynamics simulations. *Pure Appl. Chem.* **2004**, *76*(1), 231-240, DOI: 10.1351/pac200476010231.
- [52] Szalewicz, K., Reference module in chemistry, molecular sciences and chemical engineering: encyclopedia of physical science and technology. Academic Press: **2003**, p. 505-538.
- [53] Hwang, J.; Dial, B. E.; Li, P.; Kozik, M. E.; Smith, M. D.; Shimizu, K. D., How important are dispersion interactions to the strength of aromatic stacking interactions in solution. *Chem. Sci.* **2015**, *6*(7), 4358-4364, DOI: 10.1039/c5sc01370d.
- [54] Sherrill, C. D., Energy component analysis of  $\pi$  interactions. *Acc. Chem. Res.* **2013**, *46*(4), 1020-1028, DOI: 10.1021/ar3001124.
- [55] Ahmed, S. A.; Obi-Egbedi, N. O.; Bamgbose, J. T.; Adeogun, A. I., Solvent enhancement of electronic intensity in acridine and 9-aminoacridine. *J. Saudi Chem. Soc.* **2016**, *20*, S286-S292, DOI: 10.1016/j.jscs.2012.11.002.
- [56] Tao, J.; Tretiak, S.; Zhu, J., Absorption spectra of blue-light-emitting oligoquinolines from time-dependent density functional theory. *J. Phys. Chem. B* **2008**, *112*, 13701-13710, DOI: 10.1021/jp804687j.
- [57] Worsfold, P.; Townshend, A.; Poole, C., Encyclopedia of analytical science. Elsevier: **2005**, p. 249-258.